Vacuum 84 (2010) 896–901

Contents lists available at ScienceDirect

Vacuum

journal homepage: www.elsevier.com/locate/vacuum

Study of the effect of plasma current density on the formation of titanium nitride and titanium oxynitride thin films prepared by reactive DC magnetron sputtering

P.K. Barhai [a], Neelam Kumari [a], I. Banerjee [a], S.K. Pabi [b], S.K. Mahapatra [a,*]

[a] Department of Applied Physics, Birla Institute of Technology, Mesra, Ranchi 831512, India
[b] Department of Metallurgical & Material Engineering, Indian Institute of Technology, Kharagpur 721302, India

ARTICLE INFO

Article history:
Received 15 October 2009
Received in revised form
2 December 2009
Accepted 12 December 2009

Keywords:
Titanium oxynitride
Thin film
Plasma current density

ABSTRACT

Titanium nitride and titanium oxynitride films were deposited by varying the plasma current density from 10 mA/cm^2 to 40 mA/cm^2 using DC magnetron sputtering at constant gas flow rate and deposition time. Samples were characterized by Grazing Incidence X-Ray Diffraction, XPS, Nanoindentation and colorimetric analysis. Different coloured films like golden, blue, pink and green were obtained at different current densities. At lower current density (10 mA/cm^2), golden coloured stoichiometric titanium nitride film was formed. At higher current densities (20, 30 and 40 mA/cm^2), non stoichiometric Titanium oxynitride films of colour blue, pink and green were formed respectively. The thickness of the films increased with plasma current density from 43 nm to 117 nm. It was found that the colour variation was not only due to thickness of the film but also due to oxygen atoms replacing the nitrogen positions in TiN lattice. Hardness and Young Modulus of the films were found to decrease from 17.49 GPa to 7.05 GPa and 319.58 GPa–246.77 GPa respectively with increasing plasma current density. This variation of hardness and Young Modulus of the films can be speculated due to change in crystal orientation caused by oxygen incorporation in the films. The film resistivity increased from 16.46×10^{-4} to 3.28×10^{-1} Ω cm for increasing plasma current density caused due to oxygen incorporation in the crystal lattice.

1. Introduction

TiN films due to its hardness, properties of barrier diffusion, chemical stability and attractive colours have gained importance in wide range of applications like cutting tools, MEMS, solar reflector and decorative coating etc. [1–5]. Titanium nitride and titanium oxynitride coloured films are attracted due to its consumer demands in ornament industries [6]. These films have been prepared by various chemical & physical deposition techniques but mass production of coloured films at short interval is a challenging task for this industry. Titanium nitride and oxynitride film is not only important for its colour but also important for electrical properties at interface between two layers. Recent work on titanium nitride films show low electrical resistivity and also good ohmic contacts to silicon [7–9], whereas titanium oxynitride films provide a retarding diffusion barrier at the interface between a metal and silicon. It mainly occurs due to blocking of fast diffusion path by oxygen, which is leaving strong influence on the barrier performance [10]. If we could control the amount of oxygen inside the titanium nitride film, it will fulfill to the desired requirement in different industries. Hence in this work one attempt has been made to incorporate oxygen in TiN film.

Literature indicates that mechanical properties, electrical properties and colours of the TiN film mostly depend on film thickness and oxygen content in the film [11–14]. A number of reports are available on the deposition of TiN & TiON films obtained by different plasma parameters. But a very few reports are available on deposition of titanium nitrides in presence of a very small amount of oxygen at deferent plasma current density.

In the present paper attempts has been made to deposit titanium nitride and oxynitride thin films under trace of oxygen available in deposition chamber using DC magnetron sputtering. The plasma current density was varied from 10 mA/cm^2 to 40 mA/cm^2, at constant gas flow rate of (Ar: N_2) and a small incorporation of oxygen for a constant deposition time. The hardness, colour and resistivity of the deposited films could be controlled by varying the plasma current density.

2. Experimental details

2.1. Deposition

A schematic diagram of the DC magnetron sputtering deposition system is shown in Fig. 1. This system consists of a vacuum chamber,

* Corresponding author.
E-mail address: skmahapatra@bitmesra.ac.in (S.K. Mahapatra).

0042-207X/$ – see front matter © 2009 Elsevier Ltd. All rights reserved.
doi:10.1016/j.vacuum.2009.12.004

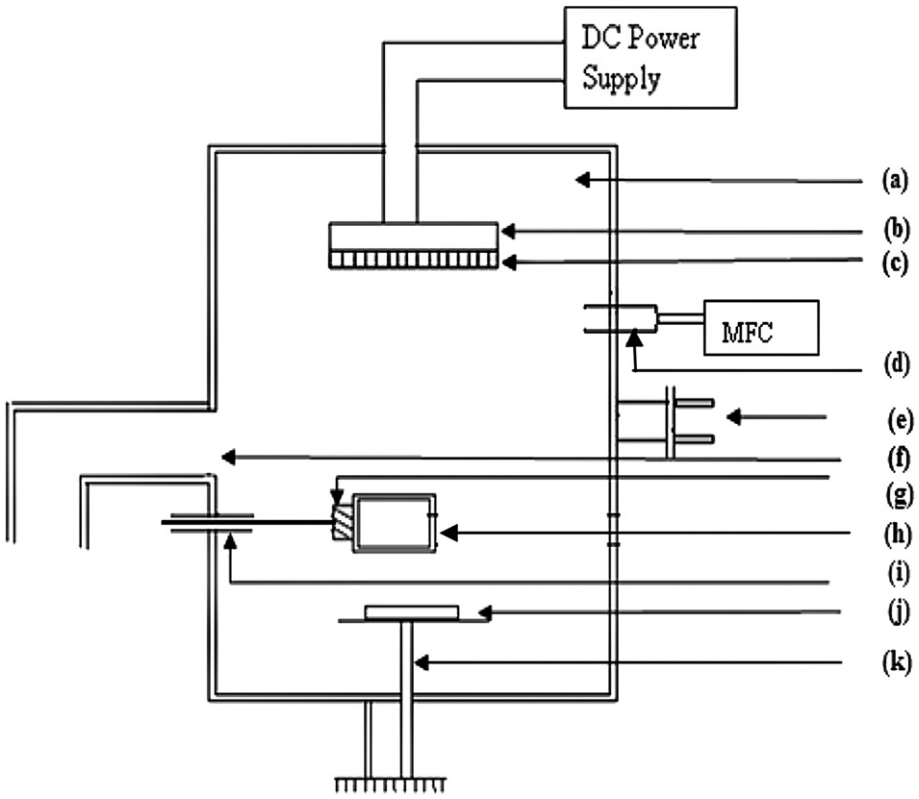

Fig. 1. Schematic Diagram of DC magnetron sputtering system (a) Vacuum chamber (b) Cathode (c) Target (d) Gas inlet through MFC (e) Pirani and Penning Gauge (f) Connected to rotary and diffusion pump (g) Insulation (h) Faraday Cup (i) Wilson seal (j) Substrate and (k) Substrate holder.

cathode, mass flow controller, sample holder, Faraday Cup and view port. Pure Ti target of size 50 mm diameters, 5 mm thick, was mechanically clamped to the magnetron cathode of the sputtering system.

Silicon substrates of size 10×10 mm^2 were obtained by cutting silicon wafers of thickness $\sim$0.5 mm. The substrates were ultrasonically cleaned and dried at room temperature prior to deposition. Silicon substrates were mounted on the sample holder and evacuated upto a base pressure of $\sim 10^{-6}$ mbar. The surface of the target was sputter etched by Ar at 100 W for 20 min to avoid contamination prior to deposition. After sputter cleaning, the argon, nitrogen and oxygen gas flow rate was maintained at 14 sccm, 6 sccm and 0.5 sccm respectively. The deposition was carried out at working pressure of $\sim 2 \times 10^{-2}$ mbar and deposition time of 1 h. In this way, four films were obtained at four different plasma current densities (10, 20, 30, 40 mA/cm^2) and constant deposition time and gas flow rates. The deposition conditions are shown in Table 1.

2.2. Measurements

2.2.1. Plasma current density

A special type of arrangement was made to measure plasma current density just before the deposition. In this arrangement a metallic rod is mounted to one end of a ceramic plate and the other end was fitted to the Faraday cup of size 20 mm $\times$ 20 mm. This ceramic plate was used to electrical isolate (electrical) Faraday cup from metallic rod. The metallic rod is passed through the Wilson seal, which is connected to one port of the deposited chamber. Before deposition, the faraday cup was aligned to plasma zone to record plasma current density. The schematic diagram of the arrangement is shown in Fig. 1.

2.2.2. Crystallinity

Crystallographic analysis of the deposited films was done by GIXRD (Model: PAN analytical X'Pertpro 3040/60). X-ray from CuK_α (wavelength 0.154 nm) was used for the measurement and operated in Bragg-Brentano geometry. GIXRD spectra of the deposited films are shown in Fig. 1.

2.2.3. Chemical compositions

XPS analysis was performed using an Omicron EIS2000, employing a hemispherical analyzer. The analyzer was operated in the constant analyzer energy (CAE) mode. The pass energy was kept at 50 and 25 eV for wide and narrow scans, and the scanning steps was 0.2 eV. The incident radiation was un-monochromated MgKα (1253.6 eV), the source running respectively at conditions of 15 KV and 20 mA. Ar^+ ion beam etching was performed using a standard ionization gun operating at 1500 eV incident energy and

Table 1
Deposition Parameters for TiN (D.C. reactive Sputtering).

Objects	Specification
Target	Ti pure (99.99%)
Substrate	Si wafer
Target to substrate distance	6.5 cm
Base pressure	1.0×10^{-6} mbar
Operating pressure	2×10^{-2} mbar
Argon	14 sccm
Nitrogen	6 sccm
Oxygen	0.5 sccm
Current density	10, 20, 30 and 40 mA/cm^2
Substrate temperature	Room Temperature, no external heating was provided
Deposition time	1 h

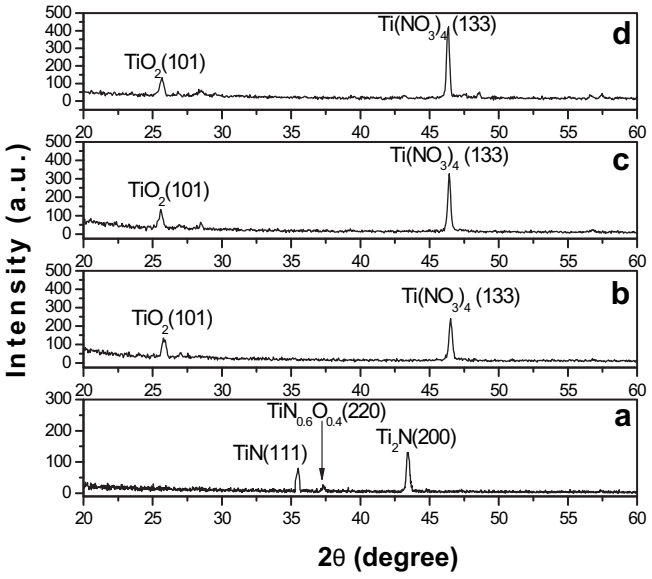

Fig. 2. GIXRD diffractograms of deposited films prepared at different current densities; (a) 10 mA/cm^2, (b) 20 mA/cm^2, (c) 30 mA/cm^2, and (d) 40 mA/cm^2.

a sample current of 6–10 μA. Core level XPS spectra of the deposited samples are shown in Fig. 3 (I) and (II).

2.2.4. Colour

Photographs of the deposited samples were taken by digital camera and shown in Fig. 4 (I). In addition to this, Colours of the samples were computed from the spectral data, acquired by a hyper spectral imaging system (Hunter Lab, USA) Colour Flex. Measurements were made against the white standard $BaSO_4$ at 10 nm intervals. Sample area of 5 × 5 mm^2 was analyzed with a spatial resolution of 12 μm/pixel. Colour specification under the standard CIE illuminant D65 was computed and represented in the CIELAB 1976 colour space for each individual pixel in the area. The average specular in the colour flex is shown in Fig. 4 (II).

2.2.5. Thickness

Thickness of the films was measured using Ellipsometer (Nano-View Inc., Korea; SEMG1000-VIS). The thickness of each sample is represented by ± 6 nm error bar shown in Table 2.

2.2.6. Hardness and Young's modulus

Hardness and Young's modulus of the deposited films were determined by low load depth sensing Nano-indenter (Nano-instruments MTS, USA). Variations of (a) Hardness and (b) Young's modulus of the deposited films is shown in Fig. 5.

2.2.7. Resistivity

The film resistivity was measured using standard four-point probe method. The resistivity was calculated using Van der Pauw method [15] according to which the resistivity is given by,

$$\rho = k \times \frac{V}{I} \times t$$

where $k = CF_1 \times CF_2$; CF_1 and CF_2 are the two geometric correction factors [15,16], V/I is the slope obtained from four-point probe voltage & currentmeasurements and t is the film thickness. In our study, the applied correction factor (k) is taken as 0.95 [17]. Variation of resistivity is shown in Fig. 6.

3. Results

3.1. GIXRD analysis

The GIXRD pattern of the films deposited at 10, 20, 30 and 40 mA/cm^2 plasma current densities are shown in Fig. 2. The crystallinity of the deposited films was confirmed using the JCPDS data tables. In Fig. 2(a) peaks observed at $2\theta = 35.31^0$, 43.41^0 and 37.20^0 correspond to (111), (200) and (220) planes of stochiometric TiN (JCPDS card No. 74-1214), Ti_2N (JCPDS card No. 77-1893) and $TiN_{0.6}O_{0.4}$ (JCPDS card No. 49-1325) respectively. Fig. 2(b)–(d), show peaks observed at $2\theta = 25.32^0$ and 46.55^0 corresponding to crystalline anatase phase of TiO_2 oriented at plane (101) (JCPDS card No. 84-1286) and Ti $(NO_3)_4$ oriented at plane (133) (JCPDS card No. 74-0948) respectively. The spectra also illustrate that the peak intensity of $Ti(NO_3)_4$ increases and gets shifted from $2\theta = 46.55$ to

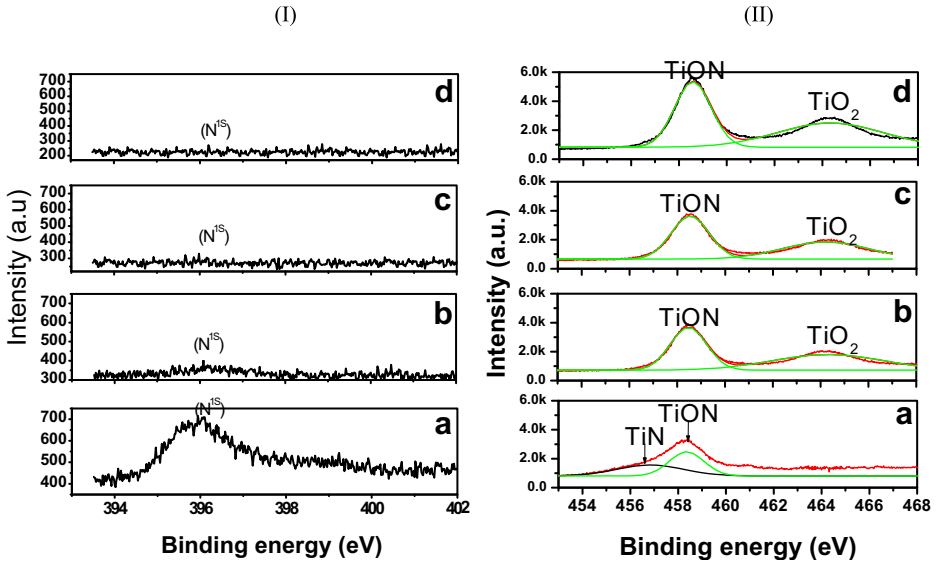

Fig. 3. (I) N^{1S} core level XPS spectra of deposited films at current densities; (a) 10 mA/cm^2, (b) 20 mA/cm^2, (c) 30 mA/cm^2, and (d) 40 mA/cm^2. 3 (II). Ti^{2P} core level XPS spectra of deposited films at current densities; (a) 10 mA/cm^2, (b) 20 mA/cm^2, (c) 30 mA/cm^2, and (d) 40 mA/cm^2.

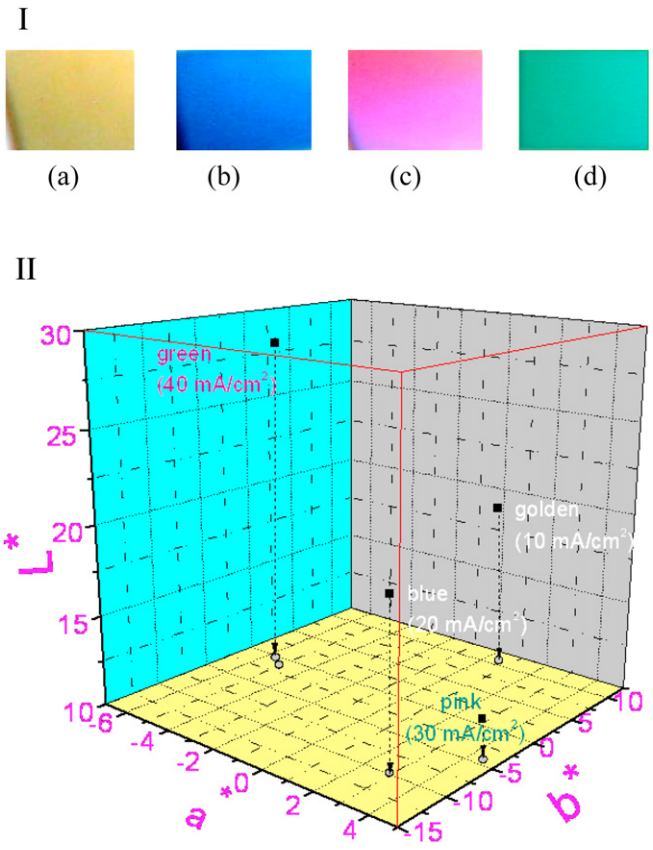

Fig. 4. (I) Colour photographs of deposited films prepared with different current densities (a) 10 mA/cm^2, golden; (b) 20 mA/cm^2, blue; (c) 30 mA/cm^2, pink and (d) 40 mA/cm^2 green. 4 (II). The average specular in the Colour Flex Hunter Lab, USA for the prepared samples with different plasma current densities; (a) 10 mA/cm^2, golden; (b) 20 mA/cm^2, blue; (c) 30 mA/cm^2, pink and (d) 40 mA/cm^2 green. Open symbols correspond to projections on a* b* plane.

$2\theta = 46.27$ with increase in plasma current density from 20 to 40 mA/cm^2. The possible formation of metastable $Ti(NO_3)_4$ compound and the XRD peak shifting may be due to the oxygen atoms most likely replacing nitrogen position in fcc TiN lattice [6,18]. Since, the Gibbs free energy for oxidation of Titanium is smaller than TiN [19,20], even the number of oxygen present inside the deposition chamber working at a vacuum $\sim 10^{-2}$ mbar is sufficient to form oxide or oxynitrides [19].

3.2. XPS analysis

The chemical compositions of the deposited films were investigated by X-Ray photoelectron spectroscopy. The N^{1s} and Ti^{2p} core level spectra of each sample deposited at different plasma current densities of 10, 20, 30 and 40 mA/cm^2 are shown in Fig. 3 (I) and (II) respectively. Fig. 3 (I) (a) shows a significant peak at 396.8 eV [14] of N^{1s} corresponding to TiN. However, N^{1s} peak shows in Fig. 3(I) (b) and (c) shows a silent feature and almost no signature in Fig. 3 (I)

Table 2
Thickness of the deposited films.

Current density (mA/cm^2)	Film Thickness (nm)
10	43
20	67
30	98
40	117

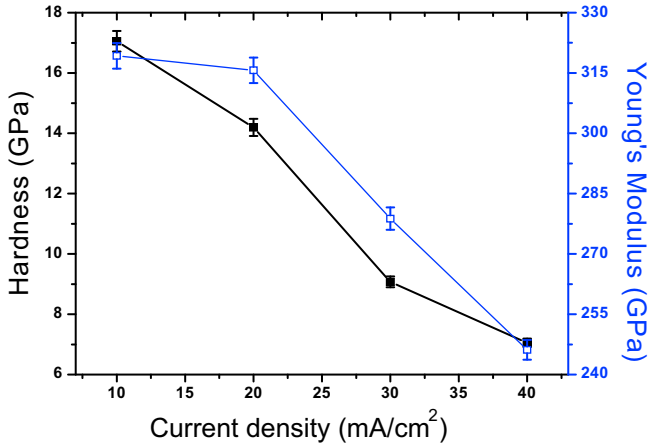

Fig. 5. Variations of (a) Hardness and (b) Young's modulus of deposited films prepared with different current densities.

(d). It indicates that nitrogen content is more on the film deposited at10 mA/cm^2 than the films deposited at 20, 30 and 40 mA/cm^2.

The Ti^{2p} core level spectra of the film deposited at 10, 20, 30 and 40 mA/cm^2, are shown in Fig. 3 (II). In Fig. 3 II (a), a broad peak is observed (ranging from 454 to 468 eV) for the sample prepared at 10 mA/cm^2. This peak was deconvoluted and fitted to two peaks at binding energies of 455.6 eV and 458.8 eV. The $Ti^{2p}{}_{3/2}$ peak at 455.6 eV corresponds to TiN [11], whereas the $Ti^{2p}{}_{1/2}$ peak at 458.8 eV corresponds to TiON [13]. It indicates the presence of titanium nitride and titanium oxynitride in the samples deposited at 10 mA/cm^2 plasma current density. Fig. 3 (II) (b, c and d) show peaks at binding energies 458.8 eV and 464.5 eV corresponding to TiON and TiO_2 [13] respectively observed from the films deposited at 20, 30 and 40 mA/cm^2. The peak intensity of TiON and TiO_2 increases with increasing current densities. The peak at 455.6 eV corresponding to TiN is absent for the films deposited at 20, 30 and 40 mA/cm^2 plasma current densities. The results indicated that stoichiometeric TiN with small impurities of oxygen was formed only in film deposited at10 mA/cm^2. It was expected since higher current density signifies for more ionization of the oxygen atoms in the plasma and forming stable oxides along with oxynitrides. It is observed that the colour of the films changes to golden, blue, pink and green as the current density changes from 10, 20 and 30–40 mA/cm^2.

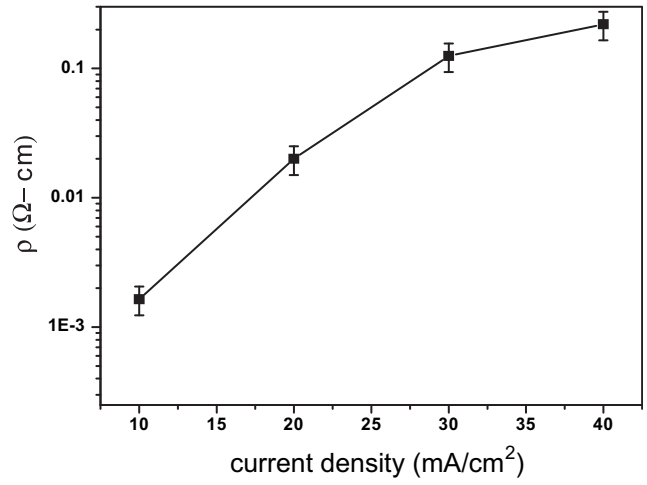

Fig. 6. The variation of the resistivity of deposited films prepared with different current densities.

Table 3
L* a*b* space colour coordinates for samples prepared at different plasma current densities.

Sample	Sample Colours	Plasma Current density (mA/cm^2)	L*	a*	b*
TiN	Golden	10	19.67 ± 1.4	0.44 ± 1.2	1.44 ± 0.7
Ti_2N, $Ti(NO_3)_4$	Blue	20	13.67 ± 1.13	−0.56 ± 1.02	−10.46 ± 0.9
Ti_2N, $Ti(NO_3)_4$	Pink	30	10.41 ± 1.06	3.16 ± 0.8	−0.14 ± 0.5
Ti_2N, $Ti(NO_3)_4$	Green	40	12.9 ± 1.3	4.68 ± 0.9	1.86 ± 0.29

3.3. Colour characterization

The colour characterization of the thin films was carried out by colorimeter (Colour Flex Hunter Lab, USA). Table 3 shows the colour variation and the optical space colour coordinates (L*, a* and b*) of the prepared samples at different current densities corresponding to areas of 5 × 5 mm^2 and spectral resolution of 10 nm. The photographs of respective coloured films deposited at different current densities are shown in Fig. 4(I). The actual colours of the films are well in agreement with the positions in the colour space coordinates as determined from colorimetric analysis. Fig. 4(II) shows the average colour in 3D colour space coordinate for the samples deposited at four different current densities. Low plasma current density (10 mA/cm^2) produced golden coloured films, whereas, with increase of the current densities (20, 30 and 40 mA/cm^2) colour of the films changed from blue, pink and then to dark green. In addition the film thickness was also found to vary from 43 nm to 117 nm [Table 2] due to current densities. It is observed that low oxygen content in the films have a bright yellow colour (golden) which gradually changes to blue, pink and green as its oxygen content increases. But thickness is also thought to affect the colour of the films [8].

According to the report of Y. L. Jayachandra et al. [11] only golden colour of the titanium nitride films was observed for the film thickness varying between 82 and 160 nm. However, the colour variation (golden to green) observed in the present films corresponds to their respective film thickness varying from ~45 to 120 nm. This observation helped to conclude that apart from the film thickness oxygen contained in the film plays dominant role in the respective colour variation of the present deposited films [8]. XPS results indicated a good correlation between oxygen incorporation in the TiN films with their respective colours. The results indicate that the change in colour of the films is interferential due to change in thickness along with oxygen content in the films [21,22].

3.4. Nano-hardness

The variation of hardness and Young's modulus of the deposited films is shown in Fig. 5. It shows that the hardness decreases from 17.49 GPa to 7.05 GPa and Young's modulus decreases from 319.58 GPa to 246.77 GPa with increase in current density from 10 mA/cm^2 to 40 mA/cm^2. The variation of hardness & Young's modulus of the as deposited films can be explained in terms crystal orientation changes due to variation of oxygen content in the films. It is well known that the TiN films having a (111) preferred orientation possess maximum hardness in comparison to any other orientation [23]. Hence, hardness decreases in the film deposited at current density due to increase of oxynitrides compounds [13,24], which changes the crystal. The XRD and XPS data in (Fig. 2) and (Fig. 3) show that the TiN (111) orientation is obtained only in the

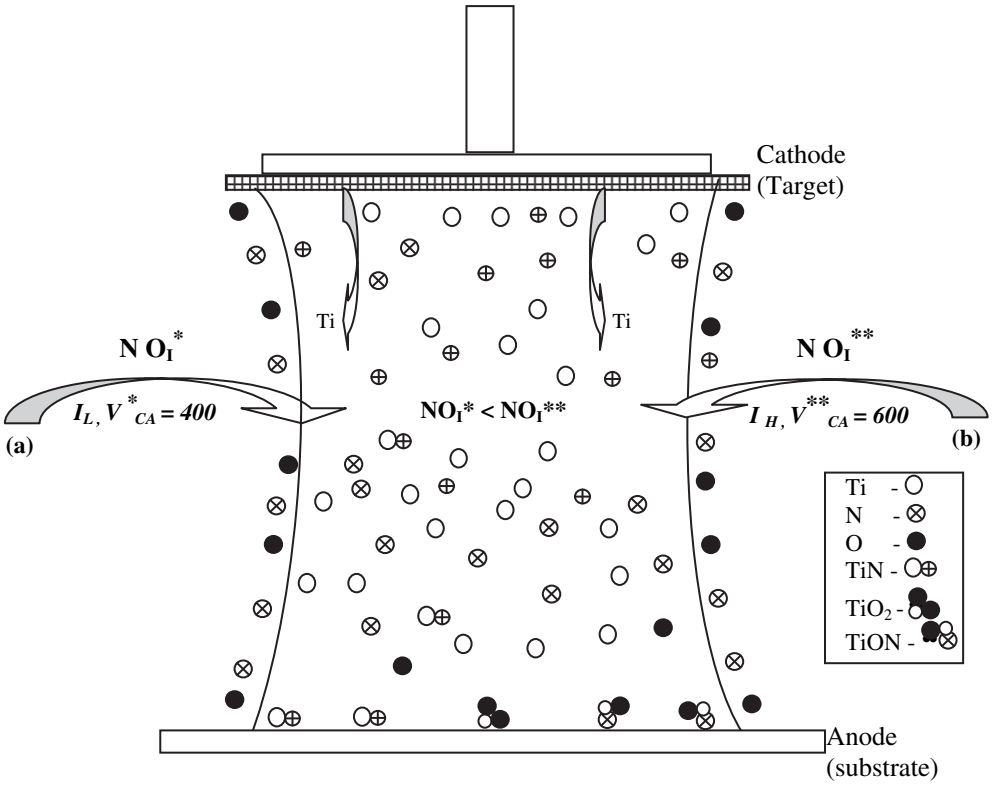

Fig. 7. Mechanism of deposited thin film at different current densities. (a) At low current (I_L), cathode to anode voltage (V^*_{CA} = 400 V), number of ionized oxygen atoms inside plasma zone (NO^*_I). (b) At high current (I_H), cathode to anode voltage (V^{**}_{CA} = 600 V), number of ionization oxygen atoms inside plasma zone (NO^{**}_I).

low current density (10 mA/cm^2) whereas oxides and oxynitrides are formed for higher current densities.

3.5. Resistivity

The variation of the resistivity of the films with the current density is shown in Fig. 6 plotted in log scale. It shows that the resistivity increases from 16.46×10^{-4} to 3.28×10^{-1} Ω cm with increase in current densities. This is expected as in accordance of the increase in oxygen content in the film. TiN along with very less amount of oxynitride produced at 10 mA/cm^2 is semiconductor having less resistivity, where as, with increase in current density the oxygen incorporation in the films increases which enhance the ceramic property of the films [9,25]. Hence the resistivity increases.

3.6. Discussions

When the atoms get sputtered out from the Ti target, the atoms/ions will get directed towards the anode for deposition. During their motion, the sputtered atoms/ions will react with imparted gas, nitrogen and oxygen present inside the chamber. The vapour of the compounds formed gets deposited atom by atom on the substrate through heterogeneous nucleation. The growth process is driven by the solid – vapour transformation through the heat released to the substrate [26]. The conceptual diagram of the deposition mechanism is shown in Fig. 7.

The formation of TiN, TiON and TiO_2 at lower (10 mA/cm^2) and higher (20, 30 and 40 mA/cm^2) plasma current densitiesis governed by the sputtering rate of Ti and the ionization probability of O_2 and N_2 in the reaction zone. At low current density, the percentage of sputtered Ti atoms is less and the ionization probability of oxygen (NO_I^*) present inside the plasma is also less than that at higher current density designated as (NO_I^{**}) in Fig. 7. Abundance of nitrogen and insufficient number of ionized oxygen (NO_I^*) cause the formation of TiN, TiON and not the stable TiO_2. However, at higher current densities, more Ti atoms get sputtered and the ionization probability of oxygen (NO_I^{**}) is also higher. Since, the enthalpy of formation of TiO_2 ($\triangle H_f = -944$ /mol) is much lesser than TiN ($\triangle H_f = -338$ kJ/mol) [27,28] and also that the availability of ionized oxygen is more at higher current density, the oxides are more readily formed at higher current densities.

4. Conclusions

Titanium nitride and titanium oxynitride coloured films were prepared at different plasma current densities using DC magnetron sputtering system at a constant gas flow rate and deposition time. It is observed that the change in colour of the films is interferential due to change in thickness along with oxygen content in the films. It could be speculated that the variation in the hardness of the films was due to the change in the crystal orientation on account of oxygen incorporation in the films. The oxygen content in the films was also found to be responsible for the change in resistivity. The results indicate that optimization of the plasma current density can produce of controlled hardness, resistivity and colour of titanium nitride and oxynitride films.

Acknowledgements

We also express our gratitude to the Administration of Birla Institute of Technology, Mesra, Ranchi, for providing the necessary facility and support for the present work. The authors also want to acknowledge Dr. Phanse and Mr. Pankaj Sagdeo for the XPS study of the films reported in this paper.

References

[1] Al-Jaroudi MY, Hentezell HTG, Homstrom SE, Bengstom A. Thin Solid Films 1990;190:265.
[2] Valvoda V, Kuzel R, Cerany R, Musil J. Thin Solid Films 1988;156:53.
[3] Kim NY, Son YB, Oh JH, Hwangbo CK, Park MC. Surf Coat Technol 2000;128–129:156.
[4] Mitter C, Komenda J, Losbichler P, Schmölz P, Werner WSM, Störi H. Vacuum 1995;46:1281.
[5] Zega B, Kornmann M, Amiguet J. Thin Solid Films 1977;45:577.
[6] Vaz F, Cerqueira P, Nascimenqu SMC, Alves E, Goudeau Ph, Riviere JP. Surf Coat Technol 2003;174–175:197.
[7] Nose M, Nagae T, Yokota M, Saji S, Zhou M, Nakada M. Surf Coat Technol 1999;116–119:296.
[8] Kumar N, Mc Ginn JT, Pourrezaei K, Lee B, Douglas EC. J Vac Sci Technol A 1988;6:1602.
[9] Wittmer M, Noser J, Melchior H. J Appl Phys 1981;52:6659.
[10] Nicolet MA, Bartur M. J.Vac Sci Technol 1981;19:786.
[11] Jayachandran YL, Narayandass SaK, Mangalaraj D, Areva Sami, Mielczarski JA. Mat Sc Eng A 2007;445–446:223.
[12] Barshilia HC, Rajam KS. Bull Mater Sci 2004;27:35.
[13] Braic M, Balaceanu M, Vladescu A, Kiss A, Braic V, Epurescu G, et al. Appl Surf Sci 2007;253:8210.
[14] Kim KH, Lee SH. Thin Solid Films 1996;283:165.
[15] Massissel LI, Glang R. Handbook of thin solid films technology. New York: McGraw-Hill Book Company; 1970.
[16] Sinha MK, Mukherjee SK, Pathak P, Paul RK, Barhai PK. Thin Solid Films 2006;515:1753.
[17] Uhlir A. Bell Syst Tech J 1955;34:105.
[18] Lu K, Zhao YH. Nano Structured Materials 1999;12:559.
[19] Yokota K, Nakamura K, Kasuya T, Tamura S, Sugimoto T, Akamatsu K, et al. J Mater Sci 2003;38:2011.
[20] Kubaschewski O, Alcock CB. Metallurgical thermochemistry. Pergamon Oxford; 1979 [Tables].
[21] Vaz F, Cerqueira P, Rebouta L, Naascimento SMC, Alves E, Goudeau Ph, et al. Thin Solid Films 2004;447–448:449.
[22] Chappe JM, Martin N, Lintymer J, Sthal F, Terwagne G, Takdown J. Appl Surf Sci 2007;253:5312.
[23] Chou WJ, Yu GP, Huang JH. Surf Coat Technol 2002;149:7.
[24] Chappe JM, Martin N, Terwagne G, Lintymer J, Gavoille J, Takdown J. Thin Solid Films 2003;440:66.
[25] Kanamori S. Thin Solid Films 1986;136:195.
[26] Ohring M. Engineering materials science. Academic Press, ISBN 0125249950; 1995.
[27] Martin N, Sanjines R, Takadoum J, Levy F. Surf Coat Technol 2001;142–144:615.
[28] Lu CJ, Zhang J, Li ZQ. J Alloys Compd 2004;381:278.